

PAPER

High-performance flexible UV photodetector based on self-supporting ZnO nano-networks fabricated by substrate-free chemical vapor deposition

To cite this article: Zhiyao Zheng *et al* 2021 *Nanotechnology* **32** 475201

View the [article online](#) for updates and enhancements.

You may also like

- [Efficient room temperature hydrogen sensor based on UV-activated ZnO nano-network](#)

Mohit Kumar, Rahul Kumar, Saravanan Rajamani *et al.*

- [Simulation, synthesis and band-gap engineering of 2nd group doped ZnO nanostructures](#)

Ghulam Sarwar, Ammar Oad, Rida Bibi *et al.*

- [The structural and optical properties of Y \(\$Y = Al, B, Si\$ and \$Ti\$ \)-doped ZnO nano thin films from the first principles calculations](#)

Wenshu Zhang, Huijun Hu, Caili Zhang *et al.*



The Electrochemical Society
Advancing solid state & electrochemical science & technology

242nd ECS Meeting

Oct 9 – 13, 2022 • Atlanta, GA, US

Abstract submission deadline: April 8, 2022

Connect. Engage. Champion. Empower. Accelerate.

MOVE SCIENCE FORWARD



Submit your abstract



High-performance flexible UV photodetector based on self-supporting ZnO nano-networks fabricated by substrate-free chemical vapor deposition

Zhiyao Zheng^{1,2}, Kewei Liu^{1,2,*} , Xing Chen¹, Baoshi Qiao^{1,2}, Hongyu Ma^{1,2}, Deming Liu¹, Lei Liu^{1,2}  and Dezhen Shen^{1,2,*}

¹ State Key Laboratory of Luminescence and Applications, Changchun Institute of Optics, Fine Mechanics and Physics, Chinese Academy of Sciences, Changchun 130033, People's Republic of China

² Center of Materials Science and Optoelectronics Engineering, University of Chinese Academy of Sciences, Beijing 100049, People's Republic of China

E-mail: liukw@ciomp.ac.cn and shendz@ciomp.ac.cn

Received 8 April 2021, revised 4 June 2021

Accepted for publication 8 August 2021

Published 31 August 2021



Abstract

Self-supporting ZnO nano-networks have been demonstrated by a substrate-free chemical vapor deposition process for the application as flexible ultraviolet (UV) photodetector. The device shows a responsivity of $\sim 300 \text{ mA W}^{-1}$ over a wide wavelength range from 254 to 365 nm and a high UV/visible rejection ratio of more than 10^4 . More interestingly, a short 90%–10% decay time of $<0.12 \text{ s}$ can be observed in the air atmosphere, and the current can fully recover to its original dark value within 1 s after switching off the light. The quick response speed should be associated with the wire–wire junction barriers and the adsorption/desorption process of oxygen molecules on the oxygen vacancies near the surface of the ZnO. In addition, the photocurrent, the dark current and the response speed of the ZnO nano-networks flexible UV photodetector nearly stay the same under different bending conditions, suggesting the excellent photoelectric stability and repeatability. Such a simple and cheap way for fabricating self-supporting ZnO-based devices has broad application prospects in the fields of flexible and wearable electronic devices.

Supplementary material for this article is available [online](#)

Keywords: ZnO nano-networks, self-supporting, flexible ultraviolet photodetector, oxygen vacancy

(Some figures may appear in colour only in the online journal)

1. Introduction

Ultraviolet (UV) photodetectors show wide applications in flame detection, biological analysis, UV irradiation detection, environmental monitoring and space communication [1–5]. Moreover, owing to the attractive features of being flexible, portable and wearable, the flexible UV photodetectors have

attracted a great deal of interests in recent years [6–8]. As is well known, the large surface-to-volume ratio and the lower dimensionality of nanostructured materials can yield the higher light sensitivity and the fewer cracks formation under a given stress than their bulk or thin-film counterparts, which are expected to enable high-performance flexible photodetectors [9–11]. ZnO nanostructure, as one of the most widely studied materials in recent years, should be a very promising candidate for flexible UV photodetection due to its

* Authors to whom any correspondence should be addressed.

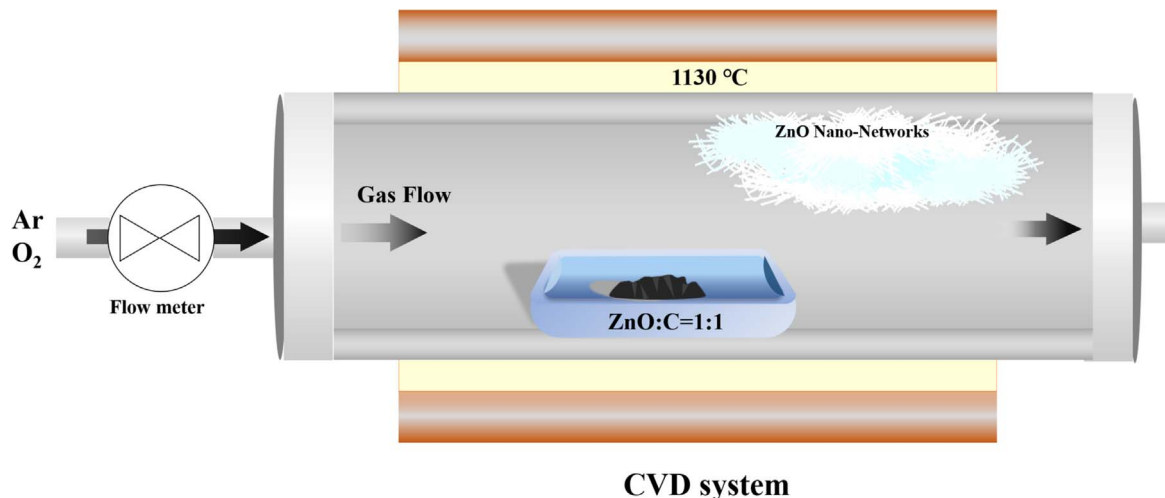


Figure 1. The schematic illustration of the preparation system of ZnO nano-networks.

large and direct band gap (~ 3.37 eV), low-cost and ease in fabrication [12–16]. Up to now, various ZnO nanostructures and their flexible UV photodetectors have been demonstrated either by gas-phase or solution-based methods [17–21]. Solution-based method is a cheap and facile way to fabricate ZnO nanostructures directly on a flexible substrate [22–27]. However, low-temperature solution-processed nanostructures often have a high density of defect states, which significantly limits their device performance and stability [28, 29]. Alternatively, gas-phase methods, including chemical vapor deposition (CVD), vacuum evaporation and sputtering, provide an effective way to produce high purity and high crystalline quality [30, 31]. However, this process usually requires high temperatures to achieve high-quality semiconductor nanostructures [32]. Therefore, to prepare flexible devices, it is usually necessary to prepare nanostructures on a high-temperature-resistant rigid substrate first, and then transfer to a flexible substrate [33–35]. This preparation process is not only relatively complicated, but also not conducive to the preparation of large-area devices.

In this work, we report self-supporting ZnO nano-networks by a substrate-free CVD process. The application of ZnO nano-networks as a flexible UV photodetector was demonstrated without any substrate. The device shows a responsivity of ~ 300 mA W⁻¹ over a wide wavelength range from 254 to 365 nm and a high UV/visible rejection ratio of more than 10⁴. More interestingly, a short decay time of <0.12 s can be observed in the air atmosphere, which should be associated with the wire–wire junction barriers and the adsorption/desorption process of oxygen molecules on the oxygen vacancies near the surface of the ZnO. In addition, the device has been tested under various bending conditions with an extremely small change in the photoelectric response characteristics, suggesting the broad application prospects in the field of flexible wearable devices.

2. Experimental details

Self-supporting ZnO nano-networks were synthesized through CVD method in a conventional horizontal tube furnace. Figure 1 shows the schematic illustration of the preparation system of ZnO nano-networks. A mixture of ZnO and graphite powders (1:1 in weight ratio) was placed in an alumina boat at the center of the tube furnace as the source materials. The temperature of the furnace was first rapidly increased to 1000 °C with a heating rate of 20 °C min⁻¹ and then continued to rise to 1130 °C with a heating rate of 5 °C min⁻¹, and maintained at this temperature for 60 min to fabricate ZnO nano-networks. High pure Ar (100 sccm) and O₂ (12 sccm) were used as the carrier gas and oxygen source, respectively. After the growth, the furnace was cooled down to room temperature naturally. Abundant self-supporting ZnO nano-networks were obtained on the tube inner wall at the downstream of the carrier gas without the presence of any substrate. To fabricate the flexible UV photodetector, we flatten the as-grown flocculent ZnO nano-networks with sulfuric acid paper, and prepare a pair of indium electrodes on it. The size of the device is about 10 mm × 10 mm × 0.4 mm (figure S1 (available online at stacks.iop.org/NANO/32/475201/mmedia)).

The morphology and structure of ZnO nano-networks were characterized by scanning electron microscopy (SEM, HITACHI S-4800), transmission electron microscopy (TEM, FEI Talos F200s) and x-ray diffraction (XRD, Bruker D8GADDS) with Cu K α radiation ($\lambda = 0.154$ nm). Photoluminescence (PL) spectra were analyzed by a fluorescence spectrophotometer (HitachiF-7000). X-ray photoelectron spectroscopy (XPS) measurements were performed using a commercial XPS spectrometer (Thermo ESCALAB 250). All the electrical characteristics were measured through a semiconductor device analyzer (Agilent B1500A). The 365 nm illumination was provided by a portable UV lamp. The

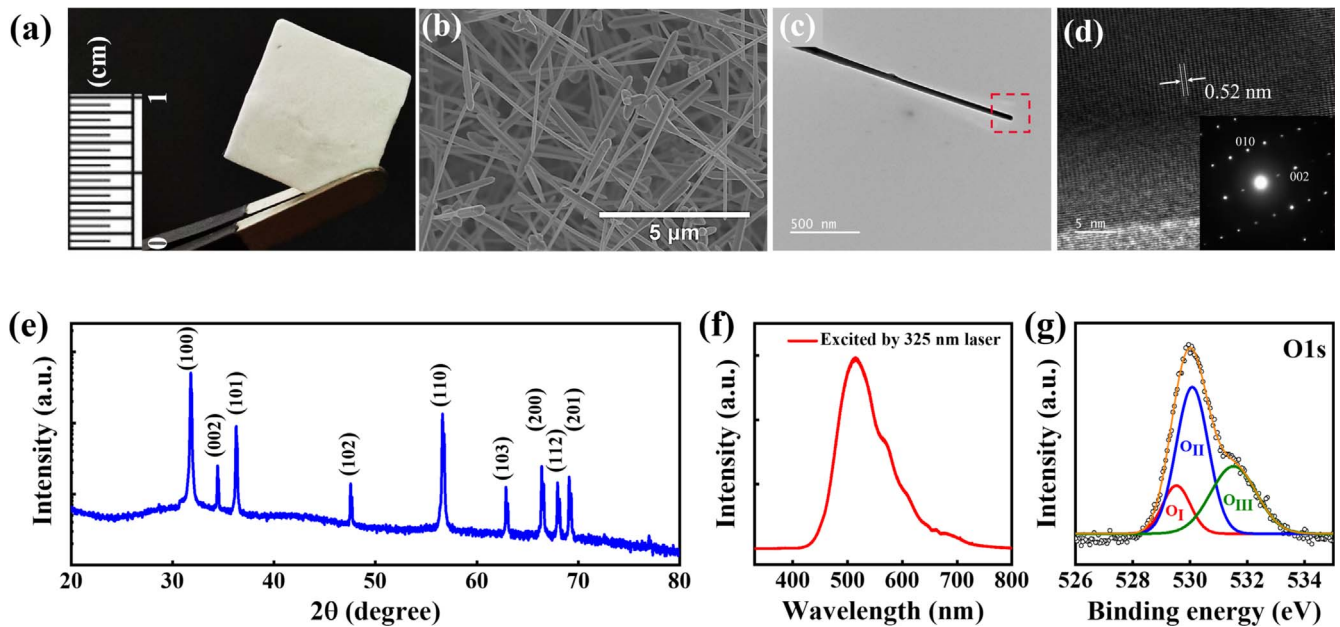


Figure 2. (a) Optical image, (b) SEM image, (c) low magnification TEM image, (d) HRTEM image and the corresponding SAED pattern (inset), (e) XRD pattern, (f) PL spectrum and (g) O1s XPS spectrum of the flattened ZnO nano-networks.

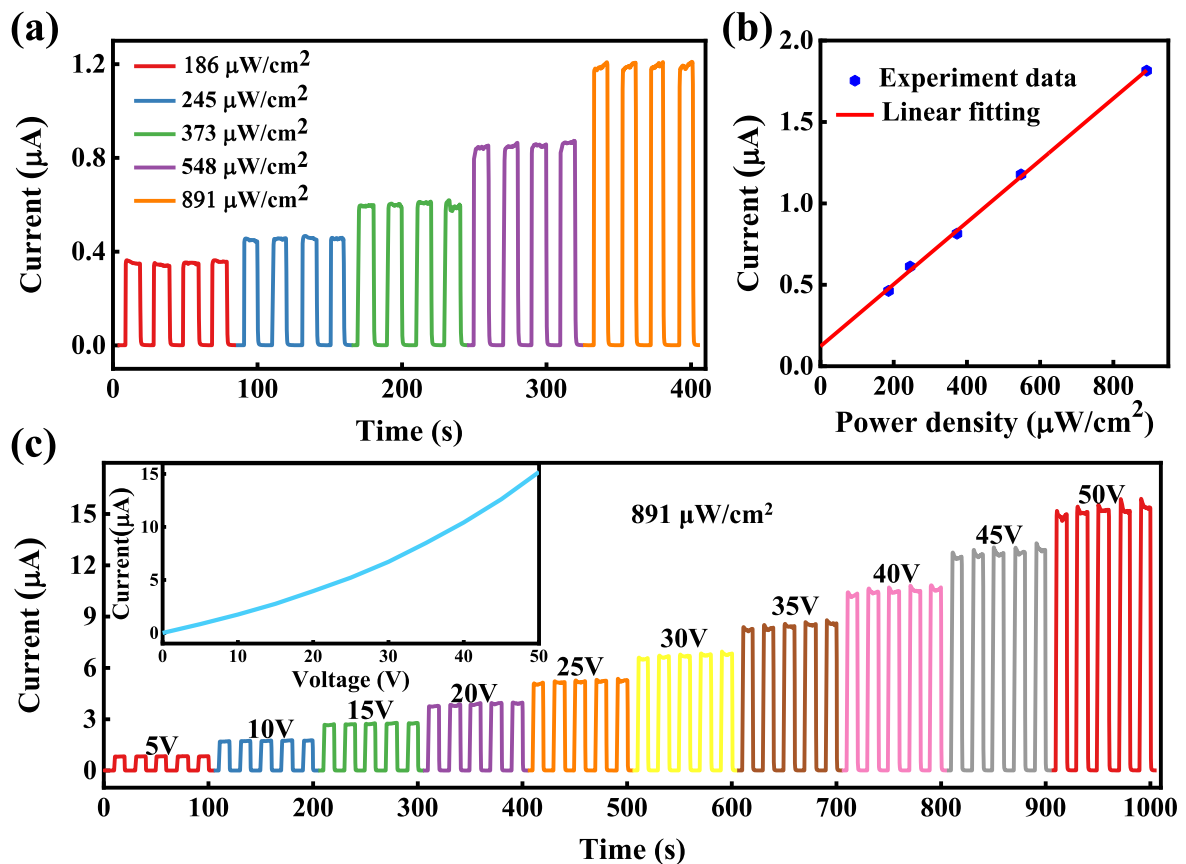


Figure 3. (a) $I-t$ curves under 365 nm illumination with different intensities biased at 5 V. (b) The photocurrent as a function of illumination intensity at 5 V. (c) The photocurrent as a function of time at different applied bias voltages under 365 nm light illumination with an intensity of $891 \mu\text{W cm}^{-2}$, and the inset is the $I-V$ curve.

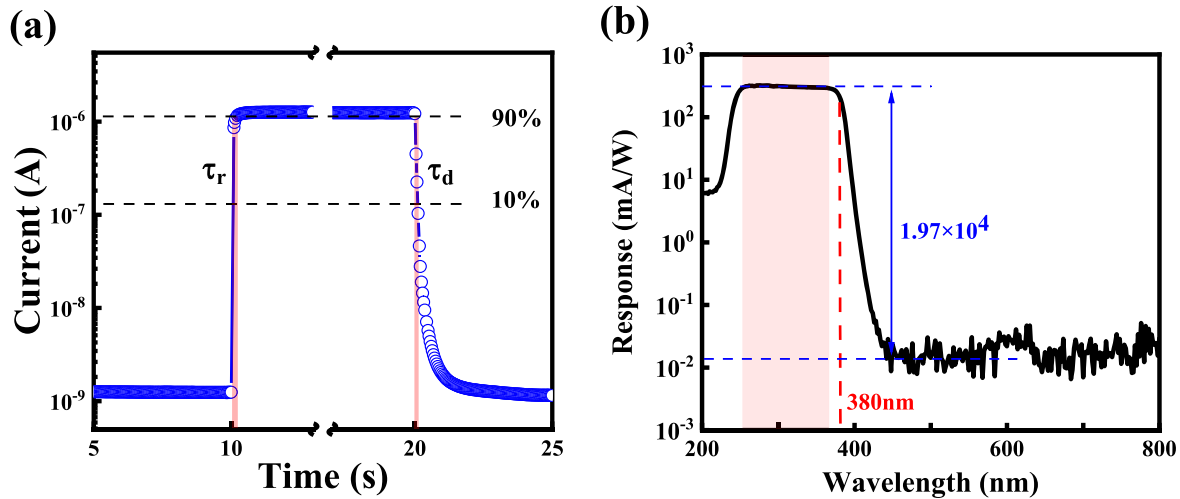


Figure 4. (a) The transient response of the ZnO nano-networks photodetector under 365 nm illumination ($891 \mu\text{W cm}^{-2}$) at 5 V. (b) The spectral response property of the device at a bias voltage of 20 V.

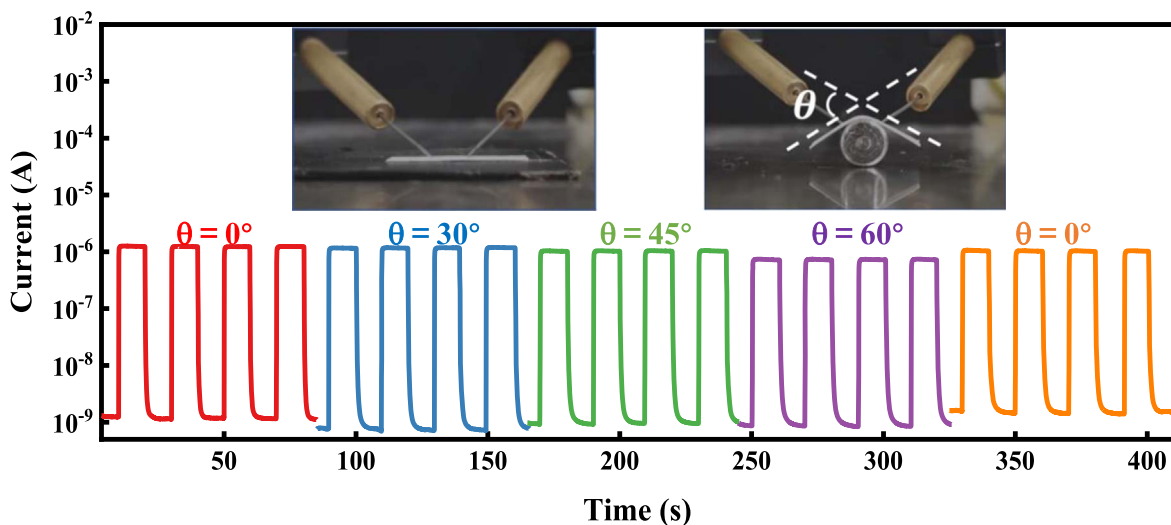


Figure 5. The on-off $I-t$ curves with different bending conditions under 365 nm UV illumination ($891 \mu\text{W cm}^{-2}$) at 5 V.

photoresponse performance was measured using a photoelectric test system equipped with an SR 830 lock-in amplifier and a 150 W Xe lamp.

3. Results and discussion

The optical image of the flattened ZnO nano-networks is showed in figure 2(a). The flattened ZnO nano-networks can behave self-supporting and intrinsically flexible property. Figure 2(b) presents the SEM image of ZnO nano-networks. It can be seen that a large quantity of freestanding nanowires were successfully synthesized with a typical diameter of 50–200 nm and a length of several tens of micrometers. Figure 2(c) shows a TEM image of a single ZnO nanowire, and figure 2(d) shows a high-resolution TEM (HRTEM) image taken from the edge of the ZnO nanowire. The distance between adjacent layers is about 0.52 nm, corresponding to (002) planes of ZnO with a hexagonal wurtzite structure.

Such results indicate that our ZnO nanowires are crystalline and grown along the c -axis. The selected area electron diffraction (SAED) image of ZnO nanowire is shown in the inset of figure 2(d). This diffraction pattern further confirms that our ZnO nanowires are single crystals with a wurtzite structure. Figure 2(e) shows the XRD pattern of the flattened ZnO nano-networks, and all the diffraction peaks can be perfectly indexed to the ZnO hexagonal wurtzite structure (JCPDS card No. 36-1451). No other diffraction peaks are observed. From the PL spectra in figure 2(f), ZnO nano-networks present a broad visible emission peak, most probably related to recombination at the defect centers such as oxygen vacancies. And almost no near band edge emission can be obtained in the UV range, further suggesting that ZnO nano-networks have large number of oxygen vacancies. High-resolution XPS spectrum of O1s is presented in figure 2(g), which can be typically deconvoluted into three types of oxygen levels: the lower bonding energy (O_I) at ~ 529.52 eV, the medium bonding energy (O_{II}) at ~ 530.08 eV, and the higher bonding

Table 1. Performance comparison of ZnO-based flexible UV photodetector.

Materials	Flexible substrate	Bias (V)	Dark current (nA)	Responsivity (A W^{-1})	UV/visible rejection	Rise time (s)	Decay time (s)	References
ZnO granular NWs	Yes	1	0.1	10^8	10^4	0.56	0.32	[40]
ZnO nanocrystals	Yes	60	0.05	0.14	10^3	0.3	0.29	[4]
Ag NP-modified ZnO	Yes	10	10	4.8×10^{-3}		3.89	1.08	[41]
Al-doped ZnO NWs	Yes	0.1	0.29	265	18.36	~100	~100	[42]
Integrated ZnO NW	Yes	3	110			—	24	[43]
ZnO/Au NP	Yes	50	—	1.51×10^5		10.3	14.2	[44]
ZnO nanorod	Yes	-2	-1.84×10^4			0.7	1.9	[45]
ZnO NWs	Yes	—	—	4.3		—	12	[46]
ZnO nanorods	Yes	5	6.44×10^3			66.4	97	[47]
Graphene/ZnO	Yes	—	—	6.27×10^{-3}		8.76	18.13	[48]
ZnO nanoparticles	Yes	5	0.04		2.3×10^4	<1	<1	[49]
ZnO nano-networks	No	5	1.2	0.3	1.97×10^4	<0.16	<0.12	This work

energy (O_{III}) at ~ 531.52 eV. In general, O_{I} , O_{II} and O_{III} can be attributed to O^{2-} within the ZnO lattice, the oxygen-deficient regions and the specific chemisorbed oxygen species, respectively. Therefore, the area ratio of $O_{\text{I}}/O_{\text{II}}$ is relatively small, indicating a higher concentration of oxygen vacancies in ZnO nano-networks.

To systematically explore the optoelectronic properties of the ZnO nano-networks UV photodetector, we studied its photoresponse with incident light of various intensities, and at various voltages. The linear I - V curves in figure S2 indicate that a good ohmic contact was formed between indium electrode and ZnO. Figure 3(a) shows the photocurrent versus time (I - t) response curves of the ZnO nano-networks UV photodetector under 365 nm ultraviolet light illumination with different power densities at 5 V. With increasing the power densities from 186 to $891 \mu\text{W cm}^{-2}$, the photocurrent increases linearly (see figure 3(b)), suggesting that the number of photoexcited carriers in ZnO is determined by the illumination intensity. A good linear relationship between the photocurrent and the light power density is the fundamental of practical and miniaturization, as the illumination intensity could be calculated simply through photocurrent. In addition, I - t curves under 365 nm illumination ($891 \mu\text{W cm}^{-2}$) at different applied voltages were shown in figure 3(c). The photocurrent of the device monotonically increased with increasing the bias voltage. The I - V characteristic curve in the inset shows that the current increases super-linearly with the increase of voltage. That's because a high voltage could improve the efficiency of carrier separation and collection. Obviously, the I - t curves in figure 3 show that our ZnO nano-networks UV photodetector has excellent stability and repeatability with fast response speed.

To further examine the rise/decay time of the device accurately, the transient response of the photodetector is presented at semi-logarithmic coordinates in Figure 4(a) under 365 nm illumination ($891 \mu\text{W cm}^{-2}$). As seen from the figure 4(a), the rise time (τ_r) (from 10% to 90% of the peak value) and the decay time (τ_d) (from 90% to 10% of the peak value) is less than 0.16 s and 0.12 s, respectively. The current can fully recover to its original dark value within 1 s after turning off the light, which is much quicker than that of any other previously reported ZnO flexible UV detectors.

In addition, under different irradiation intensity and working voltage, the response/decay time of the device does not change significantly. According to the previous reports, the quick response speed in this work should be associated with the wire-wire junction barriers and the oxygen adsorption and desorption on the oxygen vacancies near the surface of ZnO nano-networks [36]. The device shows a slower response speed in vacuum as shown in figure S3.

Responsivity R can be calculated by

$$R = (I_{\text{light}} - I_{\text{dark}})/P_{\text{opt}} \cdot s,$$

where I_{light} is the current under illumination, I_{dark} is the current in dark, P_{opt} is the optical intensity, and s is the efficient area [37–39]. Figure 4(b) depicts the spectral response

property of the device at a bias voltage of 20 V and y axis is plotted on a logarithmic scale. Obviously, the spectral responsivity is reasonably flat over a wide wavelength range from 254 to 365 nm with a responsivity of $\sim 300 \text{ mA W}^{-1}$. And a sharp cutoff at the wavelength of 380 nm is in good agreement with the ZnO band gap of ~ 3.37 eV. Moreover, UV/visible rejection ratio defined as the ratio of responsivity at 350–450 nm ($R_{350 \text{ nm}}/R_{450 \text{ nm}}$) was more than four orders of magnitude, which indicates the excellent wavelength selectivity.

For a flexible device, photoelectric stability and repeatability under different bending conditions are essential. Figure 5 exhibits the I - t curves of the ZnO nano-networks flexible UV photodetector with different bending conditions at a bias voltage of 5 V. In order to safely and controllably bend our self-supporting device, we put a flexible sheet under the device as shown in the upper graph of figure 5. Here the bending angle θ was defined as the side angle between the two tangents of the flexible sheet, which can be controlled by two metal probes and a flat cylinder. Obviously, the photocurrent, the dark current and the response speed of the ZnO nano-networks flexible UV photodetector nearly stay the same at different bending angles, suggesting the excellent photoelectric stability and repeatability.

Table 1 summarizes the performances of the reported typical ZnO-based flexible UV photodetectors. Element doping or surface modification methods have been reported to improve the performance of ZnO nanostructures, but the response is still lower than expected. The UV photodetector fabricated in this work has high response speed and high UV/visible rejection ratio, and its comprehensive performance is very competitive among similar devices. More importantly, the biggest highlight of our device is that it is the only self-supporting flexible UV detector without a substrate, making it a broader application prospect.

4. Conclusions

In summary, this work represents the first demonstration of self-supporting ZnO nano-networks flexible UV photodetector. 10%–90% rise time and 90%–10% decay time are only <0.16 s and <0.12 s, respectively. And the current can completely recover to the initial dark current level within 1 s after switching off the light. The quick response speed can be attributed to the wire-wire junction barriers and the oxygen adsorption and desorption on the oxygen vacancies near the surface of ZnO nano-networks. Meanwhile, the device shows a responsivity of $\sim 300 \text{ mA W}^{-1}$ over a wide wavelength range from 254 to 365 nm with a sharp cutoff wavelength at 380 nm. A high UV/visible rejection ratio of more than 10^4 indicates the excellent wavelength selectivity. More importantly, the device shows an excellent photoelectric stability and repeatability under different bending conditions. Our findings are useful for the fabrication of low-cost substrate-free self-supporting devices, which have important application prospects in the field of flexible electronics.

Acknowledgments

This work is supported by the National Natural Science Foundation of China (62074148, 61875194, 11727902, 12074372, 11774341, 11974344, 61975204, 11804335), the 100 Talents Program of the Chinese Academy of Sciences, Youth Innovation Promotion Association, CAS (2020225).

Data availability statement

All data that support the findings of this study are included within the article (and any supplementary files).

ORCID iDs

Kewei Liu  <https://orcid.org/0000-0001-9778-4996>

Lei Liu  <https://orcid.org/0000-0002-9714-2130>

References

- [1] Ouyang W, Teng F, He J-H and Fang X 2019 Enhancing the photoelectric performance of photodetectors based on metal oxide semiconductors by charge-carrier engineering *Adv. Funct. Mater.* **29** 1807672
- [2] Wang X, Liu K, Chen X, Li B, Jiang M, Zhang Z, Zhao H and Shen D 2017 Highly wavelength-selective enhancement of responsivity in Ag nanoparticle-modified ZnO UV photodetector *ACS Appl. Mater. Interfaces* **9** 5574–9
- [3] Ouyang W, Teng F, Jiang M and Fang X 2017 ZnO film UV photodetector with enhanced performance: heterojunction with CdMoO₄ microplates and the hot electron injection effect of Au nanoparticles *Small* **13** 1702177
- [4] Dong Y, Zou Y, Song J, Li J, Han B, Shan Q, Xu L, Xue J and Zeng H 2017 An all-inkjet-printed flexible UV photodetector *Nanoscale* **9** 8580–5
- [5] Fei X, Jiang D, Zhao M and Deng R 2021 Improved responsivity of MgZnO film ultraviolet photodetectors modified with vertical arrays ZnO nanowires by light trapping effect *Nanotechnology* **32** 205401
- [6] Wang Z *et al* 2016 Highly sensitive flexible magnetic sensor based on anisotropic magnetoresistance effect *Adv. Mater.* **28** 9370–7
- [7] Khayrudinov V, Remennyi M, Raj V, Alekseev P, Matveev B, Lipsanen H and Haggren T 2020 Direct growth of light-emitting III-V nanowires on flexible plastic substrates *ACS Nano* **14** 7484–91
- [8] Khan Y, Thielens A, Muin S, Ting J, Baumbauer C and Arias A C 2020 A new frontier of printed electronics: flexible hybrid electronics *Adv. Mater.* **32** 1905279
- [9] Boruah B D, Maji A and Misra A 2017 Synergistic effect in the heterostructure of ZnCo₂O₄ and hydrogenated zinc oxide nanorods for high capacitive response *Nanoscale* **9** 9411–20
- [10] Lou Z and Shen G 2016 Flexible photodetectors based on 1D inorganic nanostructures *Adv. Sci.* **3** 1500287
- [11] Ridha N J, Alosfur F K M, Jumali M H H and Radiman S 2020 Effect of Al thickness on the structural and ethanol vapor sensing performance of ZnO porous nanostructures prepared by microwave-assisted hydrothermal method *Nanotechnology* **31** 145502
- [12] Abbas S, Kumar M, Kim D-W and Kim J 2019 Translucent photodetector with blended nanowires-metal oxide transparent selective electrode utilizing photovoltaic and pyro-phototronic coupling effect *Small* **15** 1804346
- [13] Wang P, Wang Y, Ye L, Wu M, Xie R, Wang X, Chen X, Fan Z, Wang J and Hu W 2018 Ferroelectric localized field-enhanced ZnO nanosheet ultraviolet photodetector with high sensitivity and low dark current *Small* **14** 1800492
- [14] Li F, Meng Y, Kang X, Yip S, Bu X, Zhang H and Ho J C 2020 High-mobility In and Ga co-doped ZnO nanowires for high-performance transistors and ultraviolet photodetectors *Nanoscale* **12** 16153–61
- [15] Kuang D, Cheng J, Li X, Li Y, Li M, Xu F, Xue J and Yu Z 2021 Dual-ultraviolet wavelength photodetector based on facile method fabrication of ZnO/ZnMgO core/shell nanorod arrays *J. Alloys Compd.* **860** 157917
- [16] Wojcik P M, Bastatas L D, Rajabi N, Bakharev P V and McIlroy D N 2021 The effects of sub-bandgap transitions and the defect density of states on the photocurrent response of a single ZnO-coated silica nanospire *Nanotechnology* **32** 035202
- [17] Yin J, Huang Y, Hameed S, Zhou R, Xie L and Ying Y 2020 Large scale assembly of nanomaterials: mechanisms and applications *Nanoscale* **12** 17571–89
- [18] Zhou M, Wu B, Zhang X, Cao S, Ma P, Wang K, Fan Z and Su M 2020 Preparation and UV photoelectric properties of aligned ZnO-TiO₂ and TiO₂-ZnO core-shell structured heterojunction nanotubes *ACS Appl. Mater. Interfaces* **12** 38490–8
- [19] Golshan Bafghi Z and Manavizadeh N 2020 Low power ZnO nanorod-based ultraviolet photodetector: effect of alcoholic growth precursor *Opt. Laser Technol.* **129** 106310
- [20] Mishra Y K and Adelung R 2018 ZnO tetrapod materials for functional applications *Mater. Today* **21** 631–51
- [21] Roy V A L, Djuricic A B, Chan W K, Gao J, Lui H F and Surya C 2003 Luminescent and structural properties of ZnO nanorods prepared under different conditions *Appl. Phys. Lett.* **83** 141–3
- [22] Weintraub B, Zhou Z, Li Y and Deng Y 2010 Solution synthesis of one-dimensional ZnO nanomaterials and their applications *Nanoscale* **2** 1573–87
- [23] Ghorbani L and Nasirian S 2020 Zinc oxide nanorods assisted by polyaniline network as a flexible self-powered ultraviolet photodetector: a comprehensive study *Appl. Surf. Sci.* **527** 146786
- [24] Tian Z R R, Voigt J A, Liu J, McKenzie B, McDermott M J, Rodriguez M A, Konishi H and Xu H F 2003 Complex and oriented ZnO nanostructures *Nat. Mater.* **2** 821–6
- [25] Zheng H, Jiang Y, Yang S, Zhang Y, Yan X, Hu J, Shi Y and Zou B 2020 ZnO nanorods array as light absorption antenna for high-gain UV photodetectors *J. Alloys Compd.* **812** 152158
- [26] Gu X, Liu G, Zhang M, Zhang H, Zhou J, Guo W, Chen Y and Ruan S 2014 Photovoltaic properties of Zr_xTi_{1-x}O₂ solid solution nanowire arrays *J. Nanosci. Nanotechnol.* **14** 3731–4
- [27] Xu Q, Hong R, Cheng Q, Chen X, Zhang F, Feng J and Wu Z 2018 Solution growth of crystalline ZnO thin film and its photodetector application *Physica E* **104** 16–21
- [28] Song W, Yang D, Qiu Y, Wang Q, Wu B, Zong Y and Feng Q 2019 ZnO ultraviolet photodetector based on flexible polyester fibre substrates by low-temperature hydrothermal approach *Micro Nano Lett.* **14** 215–8
- [29] Liu J, Wu W, Bai S and Qin Y 2011 Synthesis of high crystallinity ZnO nanowire array on polymer substrate and flexible fiber-based sensor *ACS Appl. Mater. Interfaces* **3** 4197–200

- [30] Young S-J *et al* 2020 Flexible ultraviolet photodetectors based on one-dimensional gallium-doped zinc oxide nanostructures *ACS Appl. Electron. Mater.* **2** 3522–9
- [31] Feng W, Gao F, Hue Y, Dai M, Li H, Wang L and Hue P 2018 High-performance and flexible photodetectors based on chemical vapor deposition grown two-dimensional In₂Se₃ nanosheets *Nanotechnology* **29** 445205
- [32] De Fazio D *et al* 2016 High responsivity, large-area graphene/MoS₂ flexible photodetectors *ACS Nano* **10** 8252–62
- [33] Sun B, Shi T, Liu Z, Wu Y, Zhou J and Liao G 2018 Large-area flexible photodetector based on atomically thin MoS₂/graphene film *Mater. Des.* **154** 1–7
- [34] Wang Z, Safdar M, Mirza M, Xu K, Wang Q, Huang Y, Wang F, Zhan X and He J 2015 High-performance flexible photodetectors based on GaTe nanosheets *Nanoscale* **7** 7252–8
- [35] Xia K *et al* 2020 CVD growth of perovskite/graphene films for high-performance flexible image sensor *Sci. Bull.* **65** 343–9
- [36] Ma H, Liu K, Cheng Z, Zheng Z, Liu Y, Zhang P, Chen X, Liu D, Liu L and Shen D 2021 Speed enhancement of ultraviolet photodetector base on ZnO quantum dots by oxygen adsorption on surface defects *J. Alloys. Compd.* **868** 159252
- [37] Mao J, Ortiz O, Wang J, Malinge A, Badia A and Kena-Cohen S 2020 Langmuir–Blodgett fabrication of large-area black phosphorus–C(60)thin films and heterojunction photodetectors *Nanoscale* **12** 19814–23
- [38] Xie C, You P, Liu Z, Li L and Yan F 2017 Ultrasensitive broadband phototransistors based on perovskite/organic-semiconductor vertical heterojunctions *Light-Sci. Appl.* **6** e17023
- [39] Li C, Wang H, Wang F, Li T, Xu M, Wang H, Wang Z, Zhan X, Hu W and Shen L 2020 Ultrafast and broadband photodetectors based on a perovskite/organic bulk heterojunction for large-dynamic-range imaging *Light-Sci. Appl.* **9** 31
- [40] Liu X, Gu L, Zhang Q, Wu J, Long Y and Fan Z 2014 All-printable band-edge modulated ZnO nanowire photodetectors with ultra-high detectivity *Nat. Commun.* **5** 4007
- [41] Wang H-C, Hong Y, Chen Z, Lao C, Lu Y, Yang Z, Zhu Y and Liu X 2020 ZnO UV photodetectors modified by Ag nanoparticles using all-inkjet-printing *Nanoscale Res. Lett.* **15** 176
- [42] Agrawal J, Dixit T, Palani I A and Singh V 2019 Development of Al doped ZnO nanowalls based flexible, ultralow voltage UV photodetector *IEEE Sens. Lett.* **3** 1–4
- [43] Bai S, Wu W, Qin Y, Cui N, Bayerl D J and Wang X 2011 High-performance integrated ZnO nanowire UV sensors on rigid and flexible substrates *Adv. Funct. Mater.* **21** 4464–9
- [44] Jin Z, Gao L, Zhou Q and Wang J 2014 High-performance flexible ultraviolet photoconductors based on solution-processed ultrathin ZnO/Au nanoparticle composite films *Sci. Rep.* **4** 4268
- [45] Kwon D-K, Lee S J and Myoung J-M 2016 High-performance flexible ZnO nanorod UV photodetectors with a network-structured Cu nanowire electrode *Nanoscale* **8** 16677–83
- [46] Nunez C G, Vilouras A, Taube Navaraj W, Liu F and Dahiya R 2018 ZnO nanowires-based flexible UV photodetector system for wearable dosimetry *IEEE Sens. J.* **18** 7881–8
- [47] Saleh Al-Khazali S M, Al-Salman H S and Hmood A 2020 Low cost flexible ultraviolet photodetector based on ZnO nanorods prepared using chemical bath deposition *Mater. Lett.* **277** 128177
- [48] Veerla R S, Sahatiya P and Badhulika S 2017 Fabrication of a flexible UV photodetector and disposable photoresponsive uric acid sensor by direct writing of ZnO pencil on paper *J. Mater. Chem. C* **5** 10231–40
- [49] Zheng Z Q, Yao J D, Wang B and Yang G W 2015 Light-controlling, flexible and transparent ethanol gas sensor based on ZnO nanoparticles for wearable devices *Sci. Rep.* **5** 11070